

Automated Quantitative Analysis of Activator Protein-2 α Subcellular Expression in Melanoma Tissue Microarrays Correlates with Survival Prediction

Aaron J. Berger,⁶ Darren W. Davis,⁵ Carmen Tellez,¹ Victor G. Prieto,² Jeffrey E. Gershenwald,^{1,3} Marcella M. Johnson,⁴ David L. Rimm,⁶ and Menashe Bar-Eli¹

Departments of ¹Cancer Biology, ²Pathology, ³Surgical Oncology, and ⁴Biostatistics and Applied Mathematics, University of Texas M.D. Anderson Cancer Center; ⁵ApoCell, Houston, Texas; and ⁶Department of Pathology, Yale University, New Haven, Connecticut

Abstract

The activator protein-2 α (AP-2) transcription factor plays a key role in regulating expression of genes involved in tumor growth and metastasis of human melanoma. We sought to assess the prognostic significance of AP-2 expression and its role in the transition of nevi to metastatic melanoma. Two cohorts were analyzed. One was a "progression" microarray containing melanoma specimens from M.D. Anderson Cancer Center representing 84 cases and the other was a retrospective cohort from Yale University representing 214 primary melanomas and 293 metastases. Analysis of total AP-2 expression using two quantitative systems [automated quantitative analysis (AQUA) and laser scanning cytometry (LSC)] revealed no correlation with diagnosis group. LSC analysis of the M.D. Anderson Cancer Center array showed that the number of cells expressing nuclear AP-2 was highest in the benign nevi group (11.85%) and significantly decreased in each phase of melanoma progression to 0.39% in the metastatic group. Both LSC and AQUA showed decreased nuclear AP-2 levels and increased cytoplasmic AP-2 that is directly proportional to progression. Neither nuclear nor cytoplasmic expression levels correlated with outcome. Intriguingly, the ratio of cytoplasmic to nuclear AP-2 predicted outcome in the entire population and in the primary tumors alone, demonstrating the power of the ratio to normalize for variations. Furthermore, the AP-2 ratio directly correlated with other clinicopathologic factors, including Breslow depth ($R = 0.334$, $P < 0.001$). We show that a high level of AP-2 expression in the cytoplasm relative to the nucleus correlates with poor prognosis and the loss of nuclear AP-2 expression is associated with malignant transformation and progression of melanoma. (Cancer Res 2005; 65(23): 11185-92)

Introduction

The incidence and mortality rate of melanoma has increased significantly over the last 50 years, with >59,000 new cases expected this year (1). This increase in incidence, combined with the lack of effective therapy for advanced melanoma, emphasizes the need to develop better markers that correlate with clinical outcome. Since the 1970s, the Breslow depth and Clark level of invasion remain the most widely used and reliable predictors of survival in primary melanoma (2, 3). However, within each stage of melanoma, there is

a significant variability in outcome. Thus, more accurate molecular markers for melanoma progression are needed to stratify and treat patients with malignant melanoma.

Previously, we have shown that the 52 kDa transcription factor activator protein 2- α (AP-2) is involved in the progression and metastasis of human melanoma through the regulation of several target genes, such as *c-KIT*, *MCAM/MUC18*, *E-cadherin*, *p21*, *PAR-1*, and *MMP-2* (4-9). The loss of AP-2 results in the suppression of endogenous AP-2 transactivator function that may inhibit melanoma cells to respond to growth and differentiation regulatory signals (10, 11). Furthermore, inactivation of AP-2 by means of dominant-negative AP-2 gene resulted in an increase of tumorigenicity and metastasis potential in primary cutaneous melanoma cells (6). Indeed, screening human melanoma cells *in vitro* for AP-2 protein expression has shown that the majority of highly metastatic cells express low levels of nuclear AP-2 (12).

Few studies have evaluated AP-2 immunohistochemical staining in melanoma prognosis (10, 13). These studies, however, were based on individual cases or on small patient cohorts using semi-quantitative methods. Manual quantification is limited by the pathologist's ability to detect low-level staining patterns with the eye, rapidly and reproducibly score on a continuous scale, and accurately quantify subcellular expression levels. In addition, the analysis of histologic sections is complicated by the fact that tumor tissue contains a heterogeneous mixture of cell types, necrotic regions, and extracellular material. Better research tools are needed to facilitate discovery of molecular markers of prognosis that reduce variability often observed using antibody-based techniques.

Tissue microarrays provide a high-throughput approach to simultaneously screen hundreds of patient samples in a uniform fashion (14, 15). Analysis of tissue arrays permit the molecular profiling of a large number of different molecules at the DNA, RNA, and protein levels that are potentially involved in tumor development and/or progression (16, 17). Microarray technology reduces the variability between specimens because all tissue cores on the slide are simultaneously exposed to the same technical conditions. Another benefit of tissue microarrays is that automated quantitative analysis systems, such as laser scanning cytometry (LSC) or automated quantitative analysis (AQUA), can be used to generate accurate, reproducible measurement of antigen levels (18-20). Consistent measurements made across thousands of cells can help identify subtle differences in expression that are not easily detectable by the human eye (21). Furthermore, quantitative analysis provides continuous scoring as opposed to pathologist-based categorical scoring. This is particularly important when validating putative prognostic markers that display large variation in expression, especially when analyzing a large cohort as in a tissue microarray.

Note: A. J. Berger, D. W. Davis, and C. Tellez contributed equally to this work.

Requests for reprints: Darren W. Davis, ApoCell, Inc., 8030 El Rio, Houston, TX 77054. Phone: 713-440-6070; Fax: 713-440-6074; E-mail: ddavis@apocell.com.

©2005 American Association for Cancer Research.

doi:10.1158/0008-5472.CAN-05-2300

Here, we report two innovative, automated quantitative analysis systems, LSC and AQUA, to measure the subcellular expression of AP-2 in two independent melanoma tissue microarrays. The LSC platform combines features of both flow and static image cytometry analysis. LSC data acquisition captures quantitative information by detecting single cell nuclei in tissue sections, eliminating the need to acquire multiple images for carrying out complex algorithms. For this study, LSC-mediated analysis of AP-2 was done by using melanoma antigen recognized by T cells 1 (MART-1) to detect melanocytic cells. MART-1 or Melan-A is a recently discovered melanocyte differentiation antigen recognized by autologous CTLs (22). The gene that encodes MART-1 is expressed in retina, skin, and melanocytic cell lines, thereby making it an ideal marker for automated detection of melanocytes (23). In this study, LSC was used to count the number of MART-1-positive cells as a function of AP-2 expression.

AQUA does not count cells but rather uses a pair of novel algorithms that allow highly reproducible analysis of target expression in subcellular compartments in tissue sections. Validation using the AQUA system has been previously reported (18). This system identifies tumor tissue within each histospot based on the expression of tissue-specific proteins (such as S100) and then evaluates the expression of target antigen, e.g., AP-2, within the tumor mask and inside user-defined subcellular compartments. Because S100 is expressed in 98% of all melanomas (24), this protein has been used to create the tumor mask in melanoma (19, 25). Recently, AQUA was used to show that HDM2 is a marker of melanoma progression and may be used to predict survival in primary lesions (19). Thus, AQUA is designed to read tissue microarrays and optimized for high-throughput quantitative analysis.

We hypothesized that AP-2 should be active in the nucleus whereas cytoplasmic expression should be associated with loss of function. Using two independent automated quantitative analysis systems, we further show herewith that the loss of AP-2 in the nucleus is a crucial event in the progression of human melanoma and that subcellular localization of AP-2 is the critical factor in predicting survival. Furthermore, we show the importance of calculating the ratio of quantitative variable scores, showing that the ratio normalizes for individual or artifactual (fixation) variations to provide more information than either quantitative variable alone.

Materials and Methods

Patients and case selection. Specimens obtained from the Department of Pathology, M. D. Anderson Cancer Center, consisted of 84 cases comprised of melanocytic lesions including 19 benign nevus; 21 dysplastic nevus; 22 primary melanoma, including superficial spreading, nodular, acral, and lentigo malignant melanoma; 27 metastatic melanoma to s.c. tissue, lymph node, and visceral organs; and 8 normal melanocyte controls. Specimens obtained from the Department of Pathology, Yale University, consisted of 214 primary melanomas, 293 metastases, 14 local recurrences, 22 nevi, and 15 cell block controls. The specimens were resected between 1959 and 1994 with a median follow-up time of 60 months. Both studies involving human tissues were approved by the Institutional Review Board at each institution.

Tissue microarray construction. Tissue sections from each block were stained with H&E and reviewed by a pathologist to define the selective areas to be punched. To preserve the original tissue block, either 0.6 mm (biopsies) or 1.0 mm (excision specimens) cylindrical cores of tissue were punched out from donor blocks. Selected tissue cores were inserted in a standard $4.5 \times 2 \times 1$ cm recipient block using a Tissue Microarrayer (Beecher Instruments, Silver Spring, MD) with an edge-to-edge distance of 0.1 or 0.15 mm.

The tissue microarrays were then cut to 5 μ m sections and placed on glass slides using an adhesive tape transfer system (Instumedics, Inc., Hackensack, NJ) with UV cross-linking. One section from each array was stained with H&E to verify the presence of diagnostic lesional cells and to facilitate case selection for LSC- and AQUA-mediated quantitative analysis. At least two cylindrical cores from each case were obtained to construct the three tissue microarrays evaluated at M. D. Anderson Cancer Center as previously described (20). Two tissue microarrays were constructed at Yale University, with cores (0.6 mm) taken from different parts of the tumor for each microarray as previously described (19).

Immunofluorescent detection of MART-1 and AP-2 for laser scanning cytometry analysis. Sections (5 μ m) were prepared from each block, deparaffinized in xylene, rehydrated in alcohol, and transferred to PBS. Antigen retrieval was done by steaming using antigen retrieval solution (DAKO, Carpinteria, CA) by boiling tissues in 10 mmol/L citrate buffer (pH 6.0) for 10 to 20 minutes followed by cooling at room temperature for 20 minutes. Next, tissues were washed thrice for 3 minutes with PBS and incubated with protein block (5% normal horse serum in PBS) for 15 minutes at room temperature. Protein block was drained and tissues were incubated with a 1:50 dilution of rabbit anti-AP-2 (Serotec, Raleigh, NC) in protein block overnight at 4°C. Tissues were washed with PBS thrice for 3 minutes. Avoiding exposure to light, tissues were incubated with a 1:400 dilution of secondary goat anti-rabbit conjugated to Alexa 488 for 2 hours at room temperature. Tissues were washed with PBS containing 0.1% Brij for 3 minutes twice and once with PBS for 3 minutes. Next, tissues were incubated with a 1:200 dilution of mouse monoclonal anti-MART-1 (DAKO) in protein block overnight at 4°C. Tissues were washed with PBS thrice for 3 minutes and then incubated with a 1:400 dilution of secondary anti-mouse conjugated to phycoerythrin. Tissues were washed with PBS thrice for 3 minutes and incubated with 1 μ g/mL propidium iodide for 10 minutes at room temperature to counterstain total cell nuclei.

Laser scanning cytometry analysis. LSC (CompuCyte Corporation, Cambridge, MA) combines flow cytometry, image analysis, and automated fluorescence microscopy to enable fluorescence-based quantitative measurements at the single cell level. The LSC consists of an Olympus BX50 fluorescent microscope and a computer-controlled optics unit coupled to an argon, HeNe, and violet laser. Multiple lasers are used to simultaneously excite different fluorochromes in cellular specimens that emit discrete wavelengths detected by a set of photomultiplier tubes. Together, these features permit the ability to generate high-content stoichiometric data on heterogeneous populations of large numbers of cells. Thus, the LSC was used very much like a fluorescent activated cell sorter to obtain three-color immunofluorescence intensity information from the tissue microarrays.

We selected each fluorochrome based on the experimental end point of the study and compatibility with the LSC. Importantly, each probe was independently tested to ensure nonoverlapping emission between filters. Propidium iodide was used as a nuclear counterstain to contour and quantify single cells within each tissue core. To determine subcellular expression of AP-2, the peripheral contouring feature was selected to simultaneously analyze the cytoplasmic versus nuclear expression level. Using the Wincyte software, argon and HeNe lasers were selected with the appropriate filters to detect red (cell nuclei), long-red (MART-1), and green (AP-2) fluorescence. Once the scan region was selected using the epifluorescent microscope, slides were scanned using a $\times 200$ objective and detector gain voltages were set so that a maximum of 50% saturation was achieved for the brightest maximum pixel event scanned for each fluorochrome. The minimum area threshold was set to optimize contouring of single cell nuclei. To determine the percentage of MART-1-positive/AP-2-positive cells, a scattergram was created to define four quadrants that determined which cells were positive. Each gate of the scattergram was set based on the fluorescent properties of the negative control sample stained with each fluorescent probe. Once each slide was scanned, the data file was replayed to determine the percentages of each cell population, e.g., MART-1-positive/AP-2-positive cells for each tissue core. AP-2-positive cells were analyzed separately for nuclear or cytoplasmic expression. The relocation feature was used to confirm positive cellular expression.

Immunofluorescent detection of S100 and AP-2 for automated quantitative analysis. The tissue microarray slide was stained as described previously (18, 19). In brief, the slides were deparaffinized by rinsing with xylene, followed by two changes of 100% ethanol and two changes of 95% ethanol. Antigen retrieval was done in a pressure cooker containing 6.5 mmol/L citrate (pH 6.0) and endogenous peroxidase activity was blocked with 2.5% hydrogen peroxide in methanol for 30 minutes at room temperature. The slide was washed with TBS, incubated in 0.3% bovine serum albumin (BSA)/1× and TBS for 30 minutes at room temperature to reduce nonspecific background, and then stained with a combination of rabbit anti-AP-2 (C18; 1:1600, Santa Cruz Biotechnology, Santa Cruz, CA) and mouse monoclonal anti-S100, AM058 (Biogenex, San Ramon, CA) diluted in BSA/TBS at 4°C overnight. The secondary antibodies, Alexa 546-conjugated goat anti-rabbit (1:200, Molecular Probes, Eugene, OR) plus Envision antirabbit (neat; DAKO) diluted in BSA/TBS were applied for 1 hour at room temperature. 4',6-Diamidino-2-phenylindole (DAPI) was included with the secondary antibodies to visualize nuclei. The slide was washed with BSA/TBS (thrice for 5 minutes) and then incubated with Cy5-tyramide (Perkin-Elmer Life Science Products, Boston, MA) and activated by HRP, resulting in the deposition of numerous covalently associated Cy5 dyes immediately adjacent to the horseradish peroxidase (HRP)-conjugated secondary antibody. Cy5 was used because its emission peak (red) is well outside of the green-orange spectrum of tissue autofluorescence. The slides were sealed with coverslips with an antifade-containing mounting medium (with 0.6% *n*-propyl gallate).

Automated image acquisition and analysis. The AQUA automated image acquisition and analysis was done as described previously (18). Briefly, images of the tissue microarray were captured through an Olympus BX51 microscope with automated *x*-, *y*-, and *z*-stage movement with an Olympus Motorized Reflected Fluorescence System and software (IP lab v3.60, Scanalytics, Inc., Fairfax, VA) equipped with Cooke Sencisam QE High Performance camera. Low-power images of the microarray were stitched together with multiple low-resolution images of the microarray (64 × 64 pixels) at ~7 μm resolution. Areas of tumor were distinguished from stroma and nonmelanoma tissue by creating a mask with the S100 signal tagged with Alexa 546. Expression of S100 protein was used to identify the

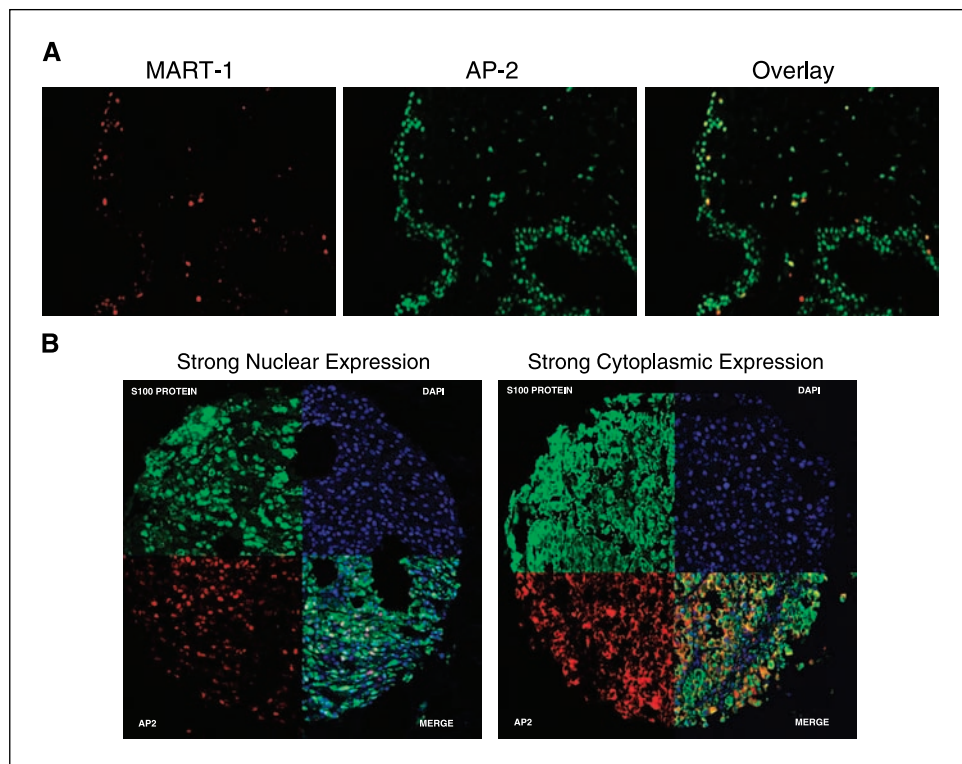
tumor mask and DAPI was used to identify the nuclear compartment. Areas of the tumor mask without DAPI were considered “nonnuclear” or “cytoplasmic.” The target marker, AP-2, was visualized with Cy5 (red). Rows and columns of the histospots were then identified, missing histospots were filled in (allowing each histospot to be identified by its coordinates), and histospots were recorded based on its position in the grid. Subsequently, monochromatic, high-resolution (1,024 × 1,024 pixel, 0.5 μm resolution) images were obtained of each histospot, both in the plane of focus and 8 μm below it, and recorded in an image stack as bitmaps. A resolution of 0.5 μm is suitable for distinguishing between large subcellular compartments such as the cell membrane/cytoplasm and nuclei. The AP-2 signal from the cytoplasmic and nuclear compartment within the S100 tumor mask was measured on a scale of 0 to 4,095 and expressed as target signal intensity relative to the respective cytoplasmic or nuclear compartment area.

Statistical analysis. The number of MART-1- and AP-2-positive cells was compared between the diagnosis groups using a Kruskal-Wallis test or a Wilcoxon rank-sum test as appropriate. The M. D. Anderson Cancer Center tissue microarray was designed to assess markers along the progression of normal melanocytic lesions to metastatic melanoma and was not designed to be a prognostic array. Therefore, subcellular localization of AP-2 expression from the Yale University tissue microarray was used to determine its association with melanoma-specific survival. The association between the consensus score and AP-2 expression and clinicopathologic variables was assessed using the χ^2 test. The prognostic significance of the clinicopathologic variables was assessed for predictive value using the univariate and multivariate Cox proportional hazards model with melanoma-specific survival as an end point. Survival curves were calculated using the Kaplan-Meier method, with significance evaluated using the Mantel-Cox log-rank test. All analyses were done using JMP or SAS (SAS Institute, Inc., Cary, NC) at a significance level of 5%.

Results

Immunofluorescent staining of melanoma tissue microarrays. Previously, we have reported that the progression of human

Figure 1. Automated detection of AP-2 in melanocytes. Tissue microarrays were immunofluorescently stained for MART-1 (A, red) or S100 and AP-2 (B, green) as described in Materials and Methods. A, a representative LSC-generated image of a case from a dysplastic nevus reveals optimization of antigen detection for MART-1 and AP-2. Colocalization of MART-1- and AP-2-positive cells appears yellow in the overlay image. Original magnification, ×200. B, representative images display tissue cores evaluated by the AQUA system for compartment-specific expression of AP-2. S100 protein (visualized under the 546 wavelength; green) defines the melanoma mask and DAPI (blue) defines the nuclear compartment. The compartment-specific AQUA scores were determined within the melanoma nuclear and melanoma nonnuclear (i.e., cytoplasmic) compartments. Note that the primary melanoma displays strong AP-2 nuclear expression (nuclear compartment, 842; cytoplasmic compartment, 270) and the metastatic melanoma core reveals strong AP-2 cytoplasmic staining (cytoplasmic compartment, 781; nuclear compartment, 490).



melanoma is associated with the loss of nuclear AP-2 expression in metastatic melanoma (5–7). Our results have been confirmed by other studies using tumor specimens (10, 13). These studies, however, were based on standard immunohistochemical analyses of total cellular AP-2 expression in primary tumors or human melanoma cell lines using semiquantitative methods.

To simultaneously measure AP-2 expression in MART-1 or S100-positive cells by LSC or AQUA, respectively, specific labeling conditions were established for optimal data acquisition. For LSC, we selected fluorescent probes that were compatible with the laser and filter configuration to minimize nonspecific emission and false-positive signals. Likewise, probes outside the spectrum of tissue autofluorescence were selected for use with the AQUA system. Tissue microarrays stained with anti-MART-1 (Fig. 1A) or S100 (Fig. 1B) and anti-AP-2 were visually inspected to verify the

quality of immunofluorescent antigen detection (Fig. 1A and B). A serial section from each tissue microarray was stained with H&E to pathologically verify the presence of diagnostic lesional cells and facilitate selection of the scan region, excluding unwanted or necrotic regions from the analysis. Tissue cores deemed uninterpretable had insufficient tumor cells in the spot, loss of tissue, or large areas of necrotic tissue.

Automated compartmental analysis of AP-2 expression in melanoma. The M. D. Anderson tissue microarray was designed to assess markers in the progression of melanoma and not prognosis. Both LSC- and AQUA-based analyses were used to characterize the subcellular expression pattern of AP-2 in each diagnosis group. Peripheral contouring capabilities of the LSC permit the simultaneous measurement of expression in the cytoplasm and nuclear compartment of each cell nuclei (Fig. 2A). Because expression of

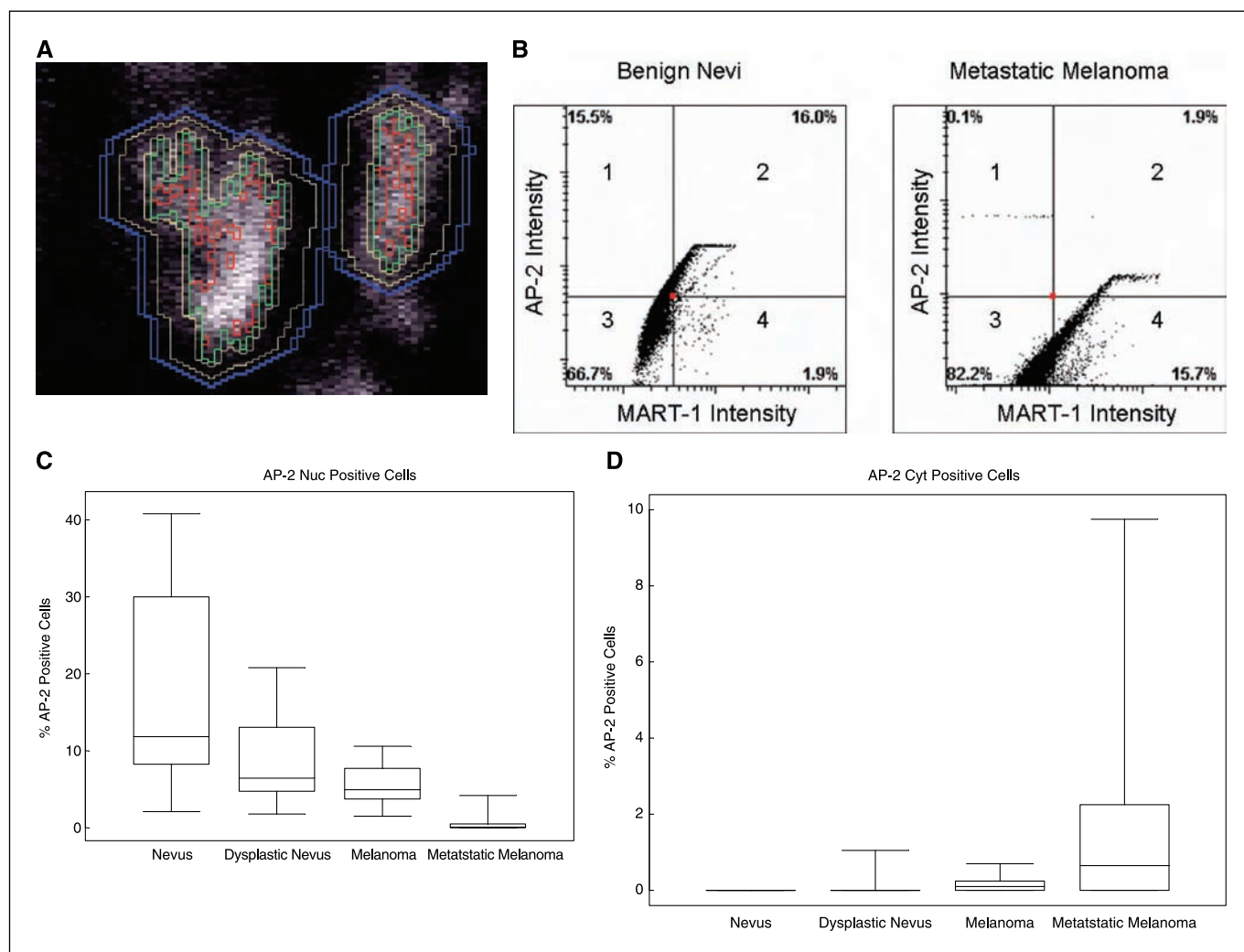


Figure 2. LSC-based quantitative analysis of subcellular AP-2 expression. *A*, LSC-mediated peripheral contour analysis. A representative LSC-scanned image of a single cell indicates the nuclear contour (red outline) and peripheral or cytoplasmic boundaries (two yellow lines). During laser scanning, quantitative information is acquired for each compartment (nuclear or cytoplasmic) based on the fluorescent intensity of each probe. Original magnification, $\times 400$; digital magnification, $\times 4$. *B*, stained tissue microarrays were scanned by LSC and individual cases from each diagnostic group were selected from the tissue map to determine the number of MART-1- and AP-2-positive cells (quadrants 2). Representative scattergrams from a benign nevus and metastatic melanoma case reveal that the percentage of MART-1-positive cells (X axis) and AP-2-positive cells (Y axis) decreased 8-fold, from 16% in the benign nevus to 1.9% in the metastatic melanoma group (quadrant 2). Gates were set based on the negative staining controls. Note that the number of MART-1-positive cells (quadrants 2 and 4) was similar between the two groups ($\sim 17\%$). *C*, nuclear expression of AP-2 from each case was analyzed. A box plot displays the median (middle line) and the minimum and maximum range (outside lines) of MART-1/AP-2-positive cells by diagnosis group. *D*, cytoplasmic expression of AP-2. Levels of AP-2 cytoplasmic expression from each case were analyzed using a Kruskal-Wallis test as described in Materials and Methods. A box plot displays the median (middle line) and the minimum and maximum range (outside lines) of MART-1/AP-2-positive cells by diagnosis group. Note that the median levels of AP-2 slightly increased with progression of melanoma.

Table 1. Characteristics of tissue cores analyzed by using LSC

Group	n	No. cells analyzed per core	No. MART-1 cells (%)*
Benign nevi	18	287 ± 402	18 ± 3.53
Dysplastic nevi	21	265 ± 196	17 ± 2.82
Melanoma	20	1,450 ± 1,082	14 ± 7.77
Metastatic melanoma	27	420 ± 315	16 ± 2.82

*No significant difference between groups.

MART-1 has been shown to be a prognostic factor for cutaneous melanoma (26), we first used the LSC to measure the number of MART-1-positive cells in each diagnostic group (Fig. 2B, quadrants 2 and 4). Importantly, three-color quantitative analysis showed no significant difference in the number of MART-1-positive cells between the benign nevi, dysplastic nevi, and primary or metastatic melanoma groups (Table 1). We, therefore, used MART-1 as a melanocytic reference for LSC-automated analysis of AP-2 in each diagnostic group. After scanning each tissue microarray, the nuclear and cytoplasmic levels of AP-2 in MART-1-positive cells were determined by selecting each case using LSC-generated coordinate position maps and replaying the data file (Fig. 2B). LSC-mediated analysis revealed a statistically significant decrease ($P < 0.0001$) in nuclear expression of AP-2 in the benign nevi group (11.85%) to a complete loss of AP-2 (0.39%) in the metastatic melanoma group (Fig. 2C). In contrast, cytoplasmic expression of AP-2 significantly increased ($P < 0.001$) with melanoma progression (Fig. 2D).

A deeper section of the same tissue microarray was analyzed by AQUA, in which S100 was used to detect the cells of melanocytic origin and DAPI was used to define the nuclear compartment. The melanoma-specific cytoplasmic compartment was defined by subtracting the DAPI image from the S100 image (after appropriate gating). Although overall expression of AP-2 tended to increase in the progression from benign nevi to malignant melanoma (Fig. 3A and B), there were significant differences in the ratio of cytoplasmic to nuclear expression relative to lesion progression. Advanced lesions showed significantly more cytoplasmic over nuclear AP-2 relative to benign nevi (Fig. 3C; Table 2).

Survival analysis and clinicopathologic correlations. The decrease in nuclear AP-2 and increase in cytoplasmic AP-2 with progression suggested that the differential expression pattern may be useful as a prognostic marker in melanoma. To assess this, we analyzed a cohort of nearly 600 cases of melanoma collected at Yale University Department of Pathology. To assess this large cohort, a second fluorescence-based system of automated analysis was used. After image acquisition for each tissue core, AQUA was done to establish the intensity of AP-2 expression per unit area within each core. Consistent with our LSC-generated results, strong nuclear AP-2 expression was noticeable in the primary melanoma cores whereas the metastatic cores displayed diffuse cytoplasmic staining (Fig. 1B). Therefore, the cytoplasmic and nuclear AP-2 expression levels generated from the Yale University tissue microarray were used to determine their potential association with melanoma-specific survival. Statistical analysis of total AP-2 expression revealed no significant association with survival (data not shown).

Hazard ratios determined by Cox univariate analysis of the AQUA scores for cytoplasmic and nuclear AP-2 expression were 1.000 [95% confidence interval (95% CI), 1.000-1.001; $P = 0.4846$] and 1.000 (95% CI, 0.999-1.000; $P = 0.2969$), respectively (Table 3). When analyses were restricted to primary melanoma specimens, the hazard ratios remained nonsignificant. In contrast, analysis of the subcellular levels of AP-2 (ratio of cytoplasmic to nuclear expression) revealed a significant association with metastases ($P < 0.01$) and survival (hazard ratio, 2.795; 95% CI, 1.609-4.857; $P = 0.0003$; Table 3). In the primary specimens, the AP-2 ratio maintained prediction of poor survival (relative risk, 4.337; 95% CI, 1.294-14.536; $P = 0.0174$; Table 3). Analysis of other clinicopathologic factors

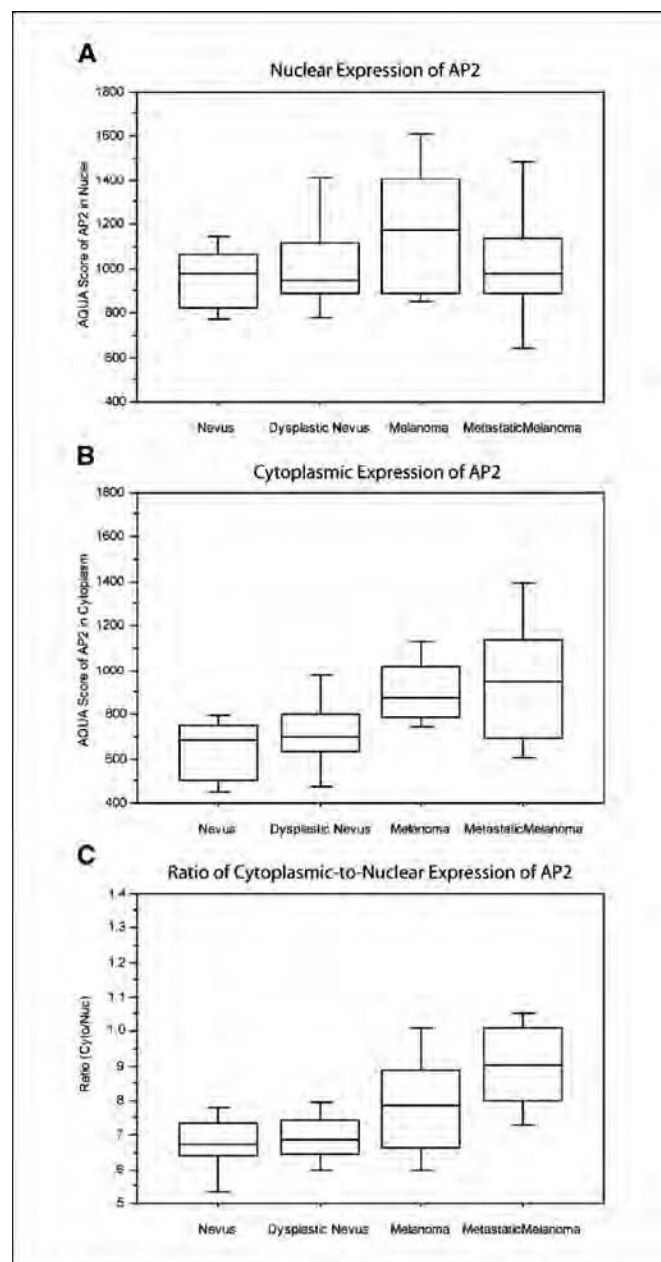


Figure 3. Box plots demonstrating the AQUA scores for compartment-specific (A, nuclear; B, cytoplasmic) expression of AP-2 measured on the progression tissue microarray as well as the ratio of cytoplasmic/nuclear expression of AP-2 (C).

Table 2. Subcellular expression of AP-2 by tissue type (measured by AQUA)

Group	n	Nucleus			Cytoplasm			Ratio		
		Mean (SE)	<i>P</i> *	<i>P</i> [†]	Mean (SE)	<i>P</i> *	<i>P</i> [†]	Mean (SE)	<i>P</i> *	<i>P</i> [†]
Benign nevi	15	942.39 (41.44)		0.1531	642.08 (38.28)		0.0007	0.68 (0.03)		<0.0001
Dysplastic nevi	13	1,032.23 (69.28)	0.2615		717.22 (50.95)	0.2419		0.70 (0.02)	0.6772	
Melanoma	16	1,185.96 (76.08)	0.1550		912.77 (42.09)	0.0059		0.80 (0.04)	0.0414	
Metastatic melanoma	23	1,041.62 (76.87)	0.2055		945.48 (69.80)	0.7213		0.91 (0.03)	0.0171	

**t* test compared with group above.

†ANOVA.

revealed that the AP-2 ratio correlated with Breslow depth ($R = 0.334$, $P < 0.001$, not shown) and was associated with microscopic satellitosis ($P = 0.0373$, not shown). Continuous AQUA scores were then divided into quartiles, based on the size of the cohort, reflecting the use of routine statistical divisions in the absence of an underlying justification for division of expression levels. Kaplan-Meier analysis of the cohort is shown in Fig. 4. Using the ratio of cytoplasmic over nuclear AP-2 shows that the ratio is highly predictive of outcome in both the total cohort (Fig. 4A) and the subset of only primary lesions (Fig. 4B). Log-rank values for each are highly statistically significant ($P < 0.0001$ and $P = 0.0094$, respectively).

To assess the independent predictive value of the AP-2 ratio, we did a multivariate analysis on the primary cutaneous lesions. In addition to the AP-2 ratio, we included the following histopathologic variables in a Cox proportional hazards model: Breslow depth, Clark level, ulceration, microscopic satellites, and tumor-infiltrating lymphocytes. The model (Table 4) shows that the AP-2 ratio maintains prognostic significance ($P = 0.0082$) after adjustment for the standard prognostic factors.

Discussion

Our goal in this study was to quantitatively assess the subcellular expression of AP-2 on a large cohort of melanoma specimens. Using two independent, automated quantitative systems to evaluate localization of AP-2 expression in two independent tissue microarrays from two separate institutions, we reached the same conclusion. To our knowledge, we show, for the first time, that the ratio of AP-2 cytoplasmic to nuclear expression pattern correlates with both progression of melanocytic lesions and with melanoma-specific survival.

Because AP-2 is a transcription factor, we hypothesized that AP-2 should be active in the nucleus, whereas cytoplasmic expression

should be associated with loss of function. Analysis of the cohort from University of Texas M. D. Anderson Cancer Center using LSC revealed almost a complete loss of AP-2 nuclear expression in the metastatic melanoma group. Our results are consistent with other studies demonstrating that AP-2 is lost in metastatic melanoma (10, 13). However, most of these studies were based on categorical scoring of total cellular expression and were not able to distinguish subtle expression patterns between cellular compartments. Application of LSC and AQUA revealed that the ratio between cytoplasmic to nuclear AP-2 expression changes with melanoma progression. Together, these data strongly suggest that translocation of AP-2 from the cytoplasm to the nucleus is disrupted during melanoma progression by an unknown mechanism. Our findings suggest that changes in subcellular AP-2 expression in melanocytes, particularly from benign nevi to dysplastic nevi (2-fold decrease), is a critical step in the genesis and progression of melanoma. Automated analysis of subcellular AP-2 expression in melanocytes may serve as a sensitive marker to monitor the progression of melanoma. It seems, therefore, that the major deficiency in AP-2 activity in metastatic melanoma is the loss of nuclear translocation. We hypothesize that this deficiency may be due to changes in the nuclear translocation signals (entry and exit) within the AP-2 protein itself, modifications in the nuclear-pore complexes, or in the activity of the transport receptors called karyopherines (or importins/exportins). In addition, we cannot exclude the possibility that anchorage of AP-2 in the cytoplasm may occur through the association with novel protein partners. Although we hypothesized that cytoplasmic AP-2 is associated with lack of function, there is the possibility that cytoplasmic AP-2 may acquire novel functions. For example, cytoplasmic accumulation of the cyclin-dependent kinase inhibitor p27Kip1 facilitates tumor progression by binding and impairing the function of the microtubule-destabilizing protein stathmin (27). The precise mechanism of actions and the identification of the AP-2 partners are currently being investigated in our laboratory.

Table 3. Cox univariate survival analysis of continuous variables

Compartmentalized AQUA score	All specimens, hazard ratio (95% CI)	<i>P</i>	Primary specimens	<i>P</i>
AP-2 in cytoplasm	1.000 (1.000-1.001)	0.4846	1.000 (0.999-1.001)	0.7540
AP-2 in nucleus	1.000 (0.999-1.000)	0.2969	1.000 (0.999-1.001)	0.4927
AP-2 ratio (cytoplasmic AP-2/nuclear AP-2)	2.795 (1.609-4.857)	0.0003	4.337 (1.294-14.536)	0.0174

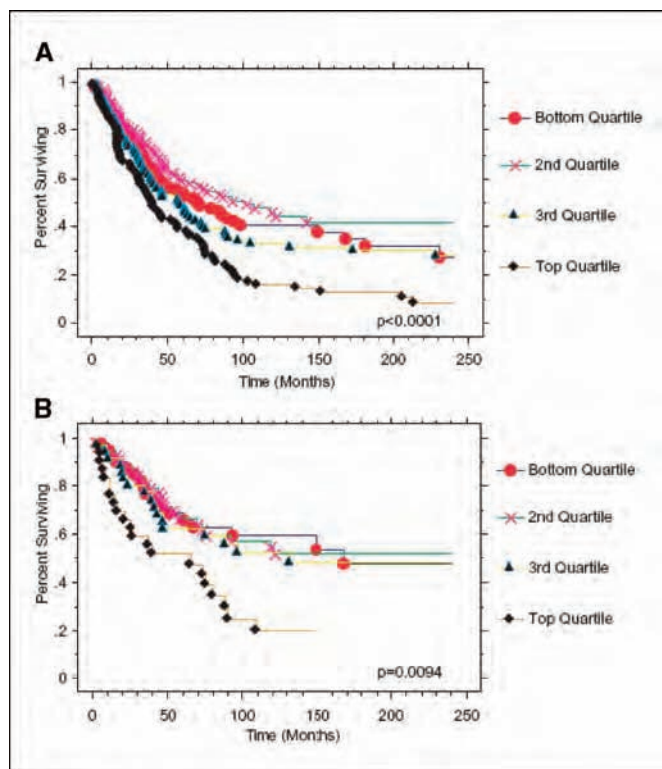


Figure 4. Melanoma tissue microarray analysis of subcellular AP-2 expression using AQUA. Kaplan-Meier survival curves were generated for AP-2 compartmental expression for the overall cohort (A) and primary melanoma (B), with time given in months, showing the four quartiles of intensities of cytoplasmic to nuclear expression.

Both the LSC and AQUA systems offer advantages for quantitative analyses of tissue microarrays that are not practical using conventional methods. In this study, we show the peripheral contouring feature of the LSC, which allows for accurate, simultaneous quantification of the number of cells with differential cytoplasmic and nuclear protein expression using multiple fluorescent probes (28). Together, these features permit investigators to evaluate the localization of a particular protein in specific cell types, e.g., AP-2 in MART-1 or S100-positive cells, in a manner that is more reproducible between tissue cores and generates consistent results in the hands of different investigators. AQUA-based quantitative analysis of AP-2 expression results in continuous scores that are directly proportional to the concentration rather than subjective pathologist-based divisions of staining into categorical scores [0-3] or "positive" and "negative." AQUA does not require laser illumination and has a higher throughput, which makes it ideal for analysis of large tissue microarrays as was shown in this study. Thus, the ability to quantify subcellular localization of markers using automated, quantitative-based systems may be crucial in assessing their potential as prognostic indicators when analyzing tissue microarrays.

To further confirm whether the changes in AP-2 subcellular expression had any potential prognostic benefit, we used the AQUA system to analyze a separate tissue microarray containing a much larger cohort of melanoma specimens from Yale University. Statistical analyses of nuclear or cytoplasmic AP-2 expression levels alone were not significantly associated with survival, suggesting that there may be case-to-case variability that obscures the overall analysis. Intriguingly, the ratio of cytoplasmic-to-nuclear

AP-2 expression levels correlated with survival, with high levels in the cytoplasm predicting an unfavorable outcome. These results illustrate the power of the ratio. Case-to-case variability, either real or artifact, is internally normalized by calculation of a ratio. It is interesting to note that only the top quartile of the ratio of cytoplasmic AP-2 to nuclear AP-2 shows significance. This may indicate some sort of threshold phenomenon, but we have no data to support this possibility. However, calculation of a ratio, although normalizing artifacts, tends to amplify subtle differences and that may be part of the reason for the appearance of this threshold effect. Future studies, including validation on other arrays and cut point optimization, are planned to better understand this observation.

Heterogeneity is often an issue that is difficult to assess but is generally addressed by repetition of the analysis with a second set of tissue cores (second fold redundancy). Indeed, these results were reproducible using a second melanoma tissue array containing different cores from the same patients, suggesting that the levels of AP-2 are homogeneously expressed throughout the tumor. Furthermore, the subcellular expression patterns of AP-2 obtained using AQUA were further confirmed by their consistency using LSC to analyze a separate cohort.

This study shows two powerful methods for automated, quantitative profiling of tissue microarrays. The automated nature of LSC- and AQUA-based technology should facilitate high-throughput molecular profiling of tissue microarrays for use in a variety of applications, such as target discovery and prognostic and diagnostic biomarker validation. When compared with conventional immunohistochemistry, these methods show the importance of quantifying expression based on fluorescence and subcellular localization. The ratio-based data would not be achievable using traditional 3,3'-diaminobenzidine-based staining methods. Thus, the LSC and AQUA systems provide a useful tool for quantitative analysis of compartmental protein expression in a reproducible fashion, free of the subjectivity associated with pathologist-based scoring.

In summary, the data presented here add further support that the loss (or cytoplasmic translocation) of nuclear AP-2 is a crucial event in the progression of melanoma. We show the importance of quantifying compartmental AP-2 expression and provide evidence that the loss of nuclear AP-2 correlates with progression in melanocytic lesions and, also, when calculated as a ratio, predicts survival.

Table 4. Multivariate survival analysis of AP-2 expression pattern and standard histopathologic variables among primary lesions

Variable	Hazard ratio (95% CI)	P
Tumor infiltrating lymphocytes (absent versus present)	3.44 (1.52-7.76)	0.003
Breslow depth (>2.00 mm versus ≤2.00 mm)	2.18 (1.11-4.25)	0.0229
Clark level (IV-V versus I-III)	1.57 (0.79-3.13)	0.2022
Ulceration (present versus absent)	1.29 (0.77-2.17)	0.3267
Microscopic satellites (present versus absent)	0.96 (0.55-1.70)	0.9003
Cytoplasmic by nuclear AP-2 ratio (top 25% versus bottom 75%)	2.14 (1.22-3.76)	0.0082

Acknowledgments

Received 7/1/2005; revised 8/24/2005; accepted 9/16/2005.

Grant support: NIH grants CA76098 and P50CA093459 (M. Bar-Eli); Commonwealth Foundation for Cancer Research (D.W. Davis); research grant CA16672 awarded by the National Cancer Institute, Department of Health and Human Services (Confocal Microscopy and Image Analysis Core Facility and Core Laboratory at M.D. Anderson Cancer Center); NIH/National Institute of General Medical Sciences Medical Scientist

Training Program grant GM07205 (A.J. Berger); and NIH grants NCI R21 CA100825 and NCI R33 CA106709 (D.L. Rimm).

The costs of publication of this article were defrayed in part by the payment of page charges. This article must therefore be hereby marked *advertisement* in accordance with 18 U.S.C. Section 1734 solely to indicate this fact.

We thank Margaret R. Spitz, MD, MPH (Chair and Professor of Epidemiology, University of Texas M.D. Anderson Cancer Center, Houston, TX), for critically reviewing the manuscript.

References

- Jemal A, Murray T, Ward E, et al. Cancer statistics, 2005. *CA Cancer J Clin* 2005;55:10–30.
- Breslow A. Thickness, cross-sectional areas and depth of invasion in the prognosis of cutaneous melanoma. *Ann Surg* 1970;172:902–8.
- Clark WH, Jr., Ainsworth AM, Bernardino EA, et al. The developmental biology of primary human malignant melanomas. *Semin Oncol* 1975;2:83–103.
- Tellez C, McCarty M, Ruiz M, Bar-Eli M. Loss of activator protein-2 α results in overexpression of protease-activated receptor-1 and correlates with the malignant phenotype of human melanoma. *J Biol Chem* 2003;278:46632–42.
- Bar-Eli M. Gene regulation in melanoma progression by the AP-2 transcription factor. *Pigment Cell Res* 2001;14:78–85.
- Gershenwald JE, Sumner W, Calderone T, et al. Dominant-negative transcription factor AP-2 augments SB-2 melanoma tumor growth *in vivo*. *Oncogene* 2001;20:3363–75.
- Jean D, Gershenwald JE, Huang S, et al. Loss of AP-2 results in up-regulation of MCAM/MUC18 and an increase in tumor growth and metastasis of human melanoma cells. *J Biol Chem* 1998;273:16501–8.
- Huang S, Luca M, Gutman M, et al. Enforced c-KIT expression renders highly metastatic human melanoma cells susceptible to stem cell factor-induced apoptosis and inhibits their tumorigenic and metastatic potential. *Oncogene* 1996;13:2339–47.
- Huang S, Jean D, Luca M, et al. Loss of AP-2 results in downregulation of c-KIT and enhancement of melanoma tumorigenicity and metastasis. *EMBO J* 1998;17:4358–69.
- Baldi A, Santini D, Battista T, et al. Expression of AP-2 transcription factor and of its downstream target genes c-kit, E-cadherin and p21 in human cutaneous melanoma. *J Cell Biochem* 2001;83:364–72.
- Nyormoi O, Wang Z, Doan D, et al. Transcription factor AP-2 α is preferentially cleaved by caspase 6 and degraded by proteasome during tumor necrosis factor α -induced apoptosis in breast cancer cells. *Mol Cell Biol* 2001;21:4856–67.
- Bar-Eli M. Molecular mechanisms of melanoma metastasis. *J Cell Physiol* 1997;173:275–8.
- Karjalainen JM, Kellokoski JK, Eskelinen MJ, et al. Downregulation of transcription factor AP-2 predicts poor survival in stage I cutaneous malignant melanoma. *J Clin Oncol* 1998;16:3584–91.
- Kononen J, Bubendorf L, Kallioniemi A, et al. Tissue microarrays for high-throughput molecular profiling of tumor specimens. *Nat Med* 1998;4:844–7.
- Rimm DL, Camp RL, Charette LA, et al. Tissue microarray: a new technology for amplification of tissue resources. *Cancer J* 2001;7:24–31.
- Cordon-Cardo C. Mutations of cell cycle regulators. Biological and clinical implications for human neoplasia. *Am J Pathol* 1995;147:545–60.
- Schraml P, Kononen J, Bubendorf L, et al. Tissue microarrays for gene amplification surveys in many different tumor types. *Clin Cancer Res* 1999;5:1966–75.
- Camp RL, Chung GG, Rimm DL. Automated subcellular localization and quantification of protein expression in tissue microarrays. *Nat Med* 2002;8:1323–7.
- Berger AJ, Camp RL, Divito KA, et al. Automated quantitative analysis of HDM2 expression in malignant melanoma shows association with early-stage disease and improved outcome. *Cancer Res* 2004;64:8767–72.
- Shen SS, Zhang PS, Eton O, Prieto VG. Analysis of protein tyrosine kinase expression in melanocytic lesions by tissue array. *J Cutan Pathol* 2003;30:539–47.
- Davis DW, Shen Y, Mullani NA, et al. Quantitative analysis of biomarkers defines an optimal biological dose for recombinant human endostatin in primary human tumors. *Clin Cancer Res* 2004;10:33–42.
- Kawakami Y, Battles JK, Kobayashi T, et al. Production of recombinant MART-1 proteins and specific anti-MART-1 polyclonal and monoclonal antibodies: use in the characterization of the human melanoma antigen MART-1. *J Immunol Methods* 1997;202:13–25.
- Coulie PG, Brichard V, Van Pel A, et al. A new gene coding for a differentiation antigen recognized by autologous cytolytic T lymphocytes on HLA-A2 melanomas. *J Exp Med* 1994;180:35–42.
- Smoller BR. Immunohistochemistry in the diagnosis of melanocytic neoplasms. *Pathology* 1994;2:371–83.
- Divito KA, Berger AJ, Camp RL, et al. Automated quantitative analysis of tissue microarrays reveals an association between high Bcl-2 expression and improved outcome in melanoma. *Cancer Res* 2004;64:8773–7.
- Berset M, Cerottini JP, Guggisberg D, et al. Expression of Melan-A/MART-1 antigen as a prognostic factor in primary cutaneous melanoma. *Int J Cancer* 2001;95:73–7.
- Baldassarre G, Belletti B, Nicoloso MS, et al. p27 (Kip1)-stathmin interaction influences sarcoma cell migration and invasion. *Cancer Cell* 2005;7:51–63.
- Davis DW, McConkey DJ, Zhang W, Herbst RS. Antiangiogenic tumor therapy. *Biotechniques* 2003;34:1048–50, 1052 passim.